Advanced Magnetic Resonance Imaging in Treated Glioblastoma Evaluation

Subjects: Neuroimaging

Contributor: Matia Martucci , Rosellina Russo , Carolina Giordano , Chiara Schiarelli , Gabriella D'Apolito , Laura Tuzza , Francesca Lisi , Giuseppe Ferrara , Francesco Schimperna , Stefania Vassalli , Rosalinda Calandrelli , Simona Gaudino

Magnetic resonance imaging (MRI) plays a key role in the evaluation of post-treatment changes, both in the immediate post-operative period and during follow-up. There are many different treatment's lines and many different neuroradiological findings according to the treatment chosen and the clinical timepoint at which MRI is performed. Structural MRI is often insufficient to correctly interpret and define treatment-related changes. For that, advanced MRI modalities, including perfusion and permeability imaging, diffusion tensor imaging, and magnetic resonance spectroscopy, are increasingly utilized in clinical practice to characterize treatment effects more comprehensively.

brain tumor imaging gliomas treatment-related changes advanced MR imaging perfusion MRI MR spectroscopy AI

1. Introduction

Glioblastoma (GB) is the most common primary malignant tumor of the central nervous system (CNS), known for its aggressive nature and limited treatment options. The National Comprehensive Cancer Network (NCCN) Guidelines provide evidence-based recommendations for its management.

The standard treatment approach for newly diagnosed GB, as outlined in the NCCN Guidelines, involves a combination of surgical resection, radiotherapy (RT), and chemotherapy with temozolomide (TMZ), commonly referred to as the Stupp protocol. Surgical resection aims to remove as much of the tumor as feasible without causing significant neurological deficits. Following surgery, RT is administered concurrently with adjuvant TMZ, which is an oral chemotherapy agent.

In cases of tumor recurrence, the treatment strategy depends on the location and extent of recurrence. If the recurrence is localized, surgical resection may be considered as an option before initiating systemic therapy.

For diffuse recurrence or cases where surgery is not feasible, systemic therapy becomes the primary treatment choice. The NCCN Guidelines suggest several preferred regimens for recurrent GB, including bevacizumab (an antiangiogenic agent), TMZ, lomustine or carmustine (chemotherapeutic agents), the PCV regimen (a combination

of procarbazine, lomustine, and vincristine), and regorafenib (a targeted therapy). The selection of the most appropriate regimen depends on various factors, including the patient's medical history, previous treatments, and performance status [1].

Magnetic resonance imaging (MRI) plays a key role in the whole clinical history of patients with GB, from the diagnosis to post-surgical evaluation and the monitoring of treatment effects. The NCCN recommends MRI immediately after surgery (up to 48–72 h), 2 to 8 weeks after RT, then every 2 to 4 months for 3 years, then every 3 to 6 months indefinitely [1].

It is well known that the neuroradiological scenario varies depending on the clinical and treatment timepoint and that structural MR imaging alone is often insufficient and unreliable to interpret and define treatment-related changes, such as the pseudophenomena (pseudoprogression and pseudoresponse) or specific drug-related MRI patterns. For that, advanced MRI modalities are increasingly utilized in clinical practice to characterize treatment effects more comprehensively. These include dynamic susceptibility contrast (DSC)- and dynamic contrast enhancement (DCE)-perfusion-weighted imaging; higher order diffusion techniques, such as diffusion tensor imaging (DTI); and MR spectroscopy (MRS).

2. Early Post-Operative Imaging in Glioblastoma

Surgery undoubtedly represents the main treatment option for patients with newly diagnosed GB, sometimes playing a crucial role even at recurrence. Surgical options at diagnosis can range from a minimally invasive biopsy to a craniotomy with the therapeutic goal of removing as much tumor tissue as safely feasible using microsurgical techniques, without compromising neurological function. The main guiding principles of brain tumor surgery are gross total resection (GTR) when appropriate, minimal surgical morbidity, and accurate diagnosis [1][2].

Several tools, including surgical navigation systems housing functional MRI or diffusion tensor imaging (DTI) datasets and intraoperative MRI, ultrasonography, functional monitoring, and fluorescence-based visualization of tumor tissue with 5-aminolevulinic acid, help in reducing post-operative residual tumor volumes while keeping the risk of new neurological deficits low [2][3].

The prognostic impact of the extent of tumor resection (EOR) is actually well established. In fact, a radical surgical approach (GTR) significantly increases survival length and quality when compared with a less radical approach (subtotal resection, STR) [4][5].

Thus, it is extremely important to determine the EOR as precisely as possible when assessing the results of surgery. Although the EOR was previously estimated by the neurosurgeons [6], it is now well recognized that the radiological detection and quantification of residual tumor is far more sensitive than intraoperative estimation [7]. MRI represents the leading imaging modality, and it is vastly superior to computed tomography (CT) in detecting residual tumor after resection [8]; CT remains an alternative in patients who cannot have an MRI (claustrophobia or unsafe implantable devices).

Time window for post-operative MR imaging has been a critical concern in recent years.

Different authors have demonstrated that an MRI obtained within the first 3 days after surgery minimized the confounding effects related to post-surgical modifications, in particular nontumoral marginal enhancement (which may mimic residual enhancing tumor), methemoglobin in the surgical bed, and eventually, tumor regrowth [6][8]. In this time window, benign enhancement related to surgical trauma is unusual, even if up to 20% of patients can show an early dural and leptomeningeal enhancement (generally near the craniotomy site or at intergyral and interlobar interfaces).

Indeed, a post-surgery baseline MRI scan should ideally be obtained within 24 to 48 h and no later than 72 h [9][10]. The rationale given for performing early post-operative MRI encompasses the assessment of the residual tumor (EOR), but also the detection of surgical complications as early as possible, as well as the availability of a baseline MRI study to plan radiotherapy and to assess treatment response (**Figure 1**) [6][7][11].

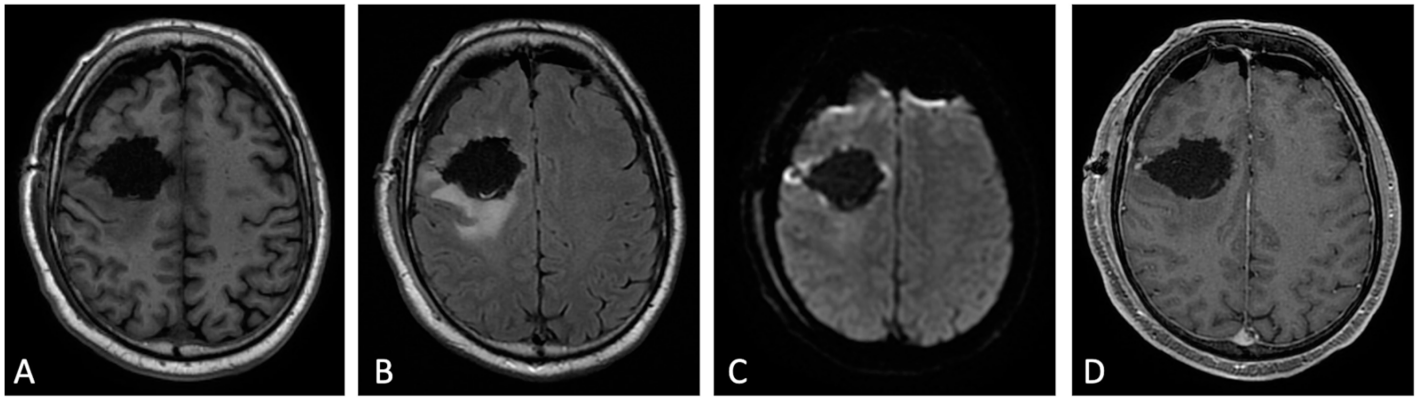

Figure 1. Early post-operative MRI. Axial pre-contrast T1w (**A**), FLAIR (**B**), DWI (**C**), and post-contrast T1w (**D**). Axial FLAIR (**B**) shows mild brain edema around the surgical site. No methemoglobin is seen on pre-contrast T1w (**A**). In DWI (**C**) a thin rim of hyperintensity (probably due to T2w- shine through effect) around the tumor cavity was attributed to post-operative change. The resection margins are free of enhancement except for a small enhancing area on the lateral aspect of surgical cavity compatible with dilated vein (**D**). Dural linear contrast enhancement could be seen in immediate post-operative scan (**D**).

A standardized MR protocol comprehensive of volumetric three-dimensional isotropic pre-contrast and post-contrast T1-weighted images, usually allows for the differentiation of the tumoral enhancement from enhancement due to the expected post-operative changes [12].

If pre-contrast and post-contrast images are carefully compared and anatomic conditions are considered, it is possible to differentiate T1 shortening due to residual enhancing tumor and early methemoglobin during the first 3 days after surgery, and to overcome several other diagnostic pitfalls affecting the evaluation of residual tumor, such as enhancement of the ependymal layer, the choroid plexus, or dilated veins at the operative site.

Uncertain findings exist, such as some kind of ultra-early contrast leakage after traumatic brain laceration. As assumed by Elster et al. [13], a variable, although not entirely predictable, enhancement might exist secondary to contrast extravasation along the fresh surgical wound.

Contrast enhancement (CE) in early post-operative MRI can be classified in three different patterns, according to Ekinci et al. [7]: thin linear (like normal dural enhancement), thick linear or thick linear-nodular enhancement (thicker than typical dural enhancement or >5 mm, with or without nodularity, respectively), or mass-like (enhancement thicker than at least 1 cm in any imaging plane). The thin linear pattern represents an expected MRI finding, whereas thick linear-nodular enhancement and mass-like appearance should be carefully reported because the first is associated with tumor regrowth, and the latter represents residual tumor (**Figure 2**) [10]. Accordingly, Garcia-Ruiz et al. demonstrated that pathological enhancement thickness on post-surgical MRI correlated with both progression-free survival (PFS) and overall survival (OS) [14].

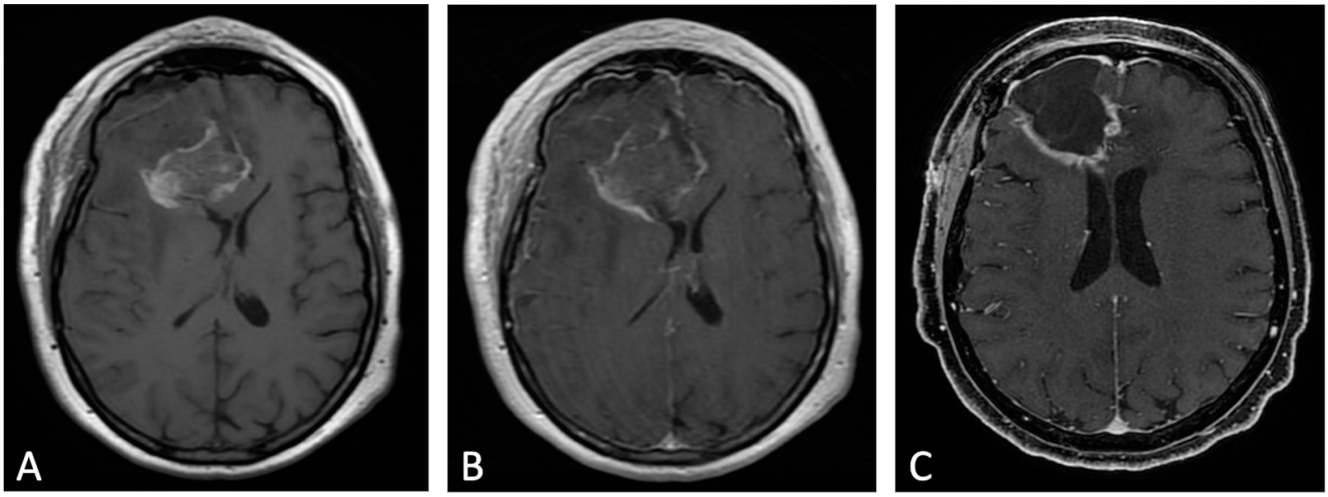

Figure 2. Example of evolution of thick linear CE. Pre-contrast (**A**) and post-contrast (**B**) T1w images of early post-operative MRI after surgical resection of GB; post-contrast T1w of MRI performed one month after surgery (**C**). Thick peripheral enhancement may be seen particularly along the medial and posterior margin of the surgical site, with obvious tumor progression consistent with an area of thick linear-nodular enhancements at the resection bed one month after surgery.

3. MRI Findings during First-Line Therapy

3.1. Stupp Protocol

The current standard of care for GB is surgical resection followed by RT and concomitant and adjuvant TMZ chemotherapy, which is named Stupp protocol after the oncologist who proposed this treatment. Specifically, the protocol includes the administration of radiotherapy to the post-operative bed (total 60 Gy–2 Gy per daily fraction from Monday to Friday over 6 weeks), and TMZ during RT (75 mg/m^2 of body surface area per day, 7 days per

week) and post-RT after a 4 week-break (adjuvant, 6 cycles consisting of 150 to 200 mg/m^2 of body surface area for 5 days during each 28-day cycle) [15].

TMZ is a second-generation alkylating chemotherapy agent absorbed after oral administration that crosses the BBB and which has a schedule-dependent antitumor activity. Its effect is based on the inactivation of MGMT (a DNA-repairing protein) and its subsequent activation of the p53 pathway that leads to apoptosis. Consequently, the identification of MGMT expression and p53 status in GB might help to identify those patients who will or will not respond to TMZ [16].

3.2. MRI during Stupp Protocol

MRI is the modality of choice for the routine follow-up of GB during the Stupp protocol to monitor the possible appearance of pathological tissue in the surgical bed and other brain areas. As is known, the appearance of signal alterations on MRI during the treatment phase is not necessarily tumor tissue; it may be post-treatment changes or, more often, the coexistence of both [17][18].

During first-line therapy and its follow-up, treatment-related complications are mainly due to radiation injury, and it is possible to separate them on the basis of their time of occurrence in [19]:

- Acute and early delayed: days to months (usually less than 3 months) following treatment, generally transient (e.g., pseudoprogression);
- Late delayed: at least 6 months after radiation and considered irreversible and progressive (e.g., radiation necrosis).

Since both true progression (TP) and treatment-related alterations have BBB disruption and vasogenic edema, the resulting MR features are T2w/FLAIR (fluid-attenuated inversion recovery) hyperintensity and contrast-enhancing areas. Thus, it remains a challenge for the radiologist to distinguish between them, or, when both are present, which one gives the predominant component.

DWI measures the diffusion of water molecules in tissues and can be useful in detecting areas of restricted diffusion, which may indicate active tumor or residual disease, as they suggest regions of higher cellularity [20]. PWI evaluates blood flow within the tumor, which can provide insights into tumor vascularity and help differentiate between treatment-related changes and tumor progression. MRS analyzes the chemical composition of tissues and can help identify the presence of specific metabolites associated with tumor cells.

By incorporating these advanced MRI sequences into the follow-up protocol, clinicians can obtain more comprehensive information about the tumor and its response to treatment. This can aid in distinguishing between post-surgical residual tumor, non-enhancing tumor, and treatment-related alterations, thereby improving the accuracy of disease assessment and progression monitoring.

3.3. Early Post-Treatment Alterations

3.3.1. Pseudoprogression: Definition and Physiopathology

Pseudoprogression (PsP) is an early-delayed treatment-related alteration (first 3 to 6 months after completion of chemoradiotherapy), radiologically defined as new or enlarging contrast-enhancing areas on follow-up MRI, which subsides or stabilizes without further treatments [21].

It occurs in approximately 20–30% of patients, and it is thought to be due to inflammatory tissue reactions and oligodendroglial injury secondary to irradiation. It may be increased by TMZ, resulting in transient vessel dilatation and permeability, and vasogenic edema [9][21][22].

PsP may or may not be associated with neurological symptoms, and it is more common in patients with methylated MGMT-promoter GBs. Moreover, some studies suggest that PsP may have a relatively good prognosis [21].

3.3.2. Imaging: Conventional and Advanced MRI Sequences:

As previously told, the hallmark of PsP is the presence of new or enlarging contrast-enhancing areas. By conventional MRI alone, it can be challenging to distinguish between TP and PsP. Advanced MRI techniques provide additional biomarkers that can improve diagnostic specificity.

DWI definitely represents the most widely used and available technique, so that it is no longer considered as advanced. Through the evaluation of DWI signal and ADC maps, it is possible to obtain crucial information on the nature of parenchymal alterations. In particular, GB usually shows restricted diffusivity and decreased ADC values due to increased cellularity. On the contrary, PsP has elevated ADC values, mainly reflecting vasogenic edema. A mean ADC value lower than 1200×10^{-6} mm^2/s is reported to be more suggestive of TP than PsP [21].

PWI often represents the key to the interpretation of MRI findings during follow-up of treated GBs. PWI includes different techniques, such as DSC and DCE (which exploit properties of exogenous gadolinium contrast medium), and arterial spin labeling (ASL), which is based on the magnetic labeling of inflowing arterial blood used as an endogenous contrast agent.

DSC is actually the most used and validated PWI technique. It is a T2*-weighted sequence that detects the susceptibility effects of contrast medium. Its main parameters are relative cerebral blood volume (rCBV), relative cerebral blood flow (rCBF), and mean transit time (MTT). Among these, rCBV (mean and maximum) allows for the discrimination of the areas of PsP (lower mean and maximum rCBV) from TP (higher mean and maximum rCBV) (**Figure 3** and **Figure 4**) [21][23].

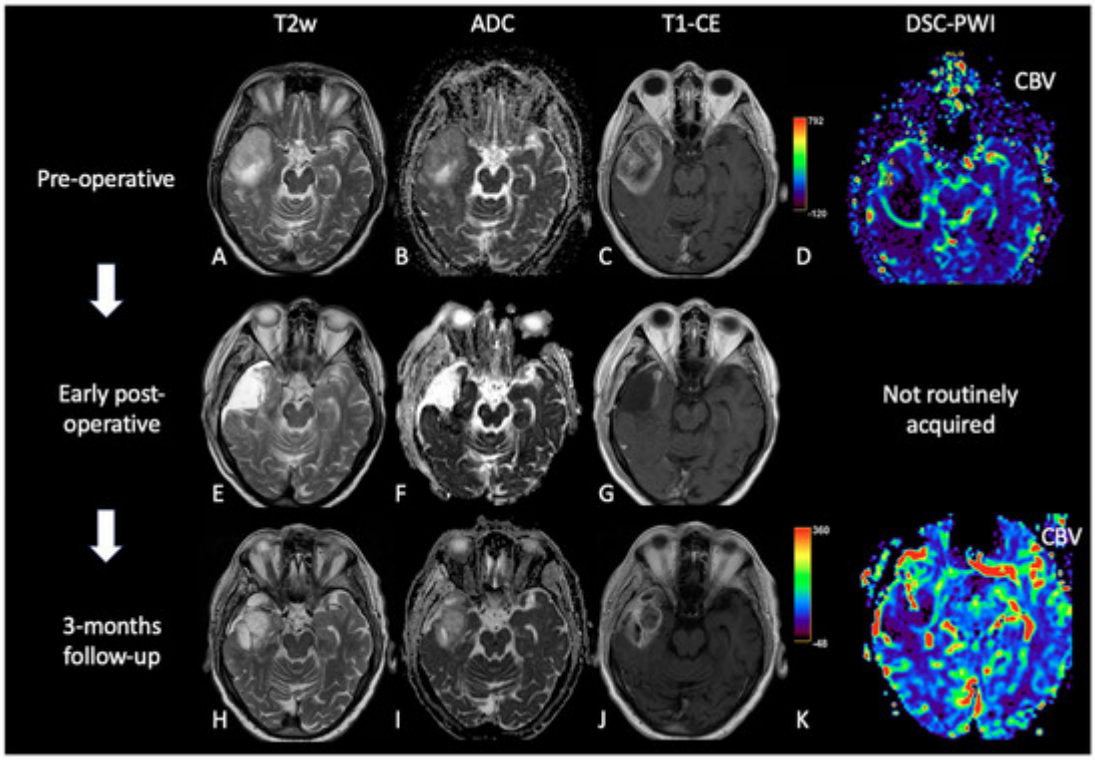

Figure 3. Case of PsP. (**A**,**E**,**H**) T2w axial images; (**B**,**F**,**I**) ADC maps; (**C**,**G**,**J**) post-contrast T1w; (**D**,**K**) DSC-CBV maps. The upper row shows a right temporal GB with low ADC (in its solid component), CE, and high perfusion values in the CBV map. In the middle row, there are post-operative images of macroscopically complete tumor resection. The lower row shows images two months after the beginning of Stupp treatment, highlighting the appearance of tissue with CE in the surgical bed, which shows increased ADC values compared to the primary tumor and without a significant increase of rCBV values, suggesting PsP.

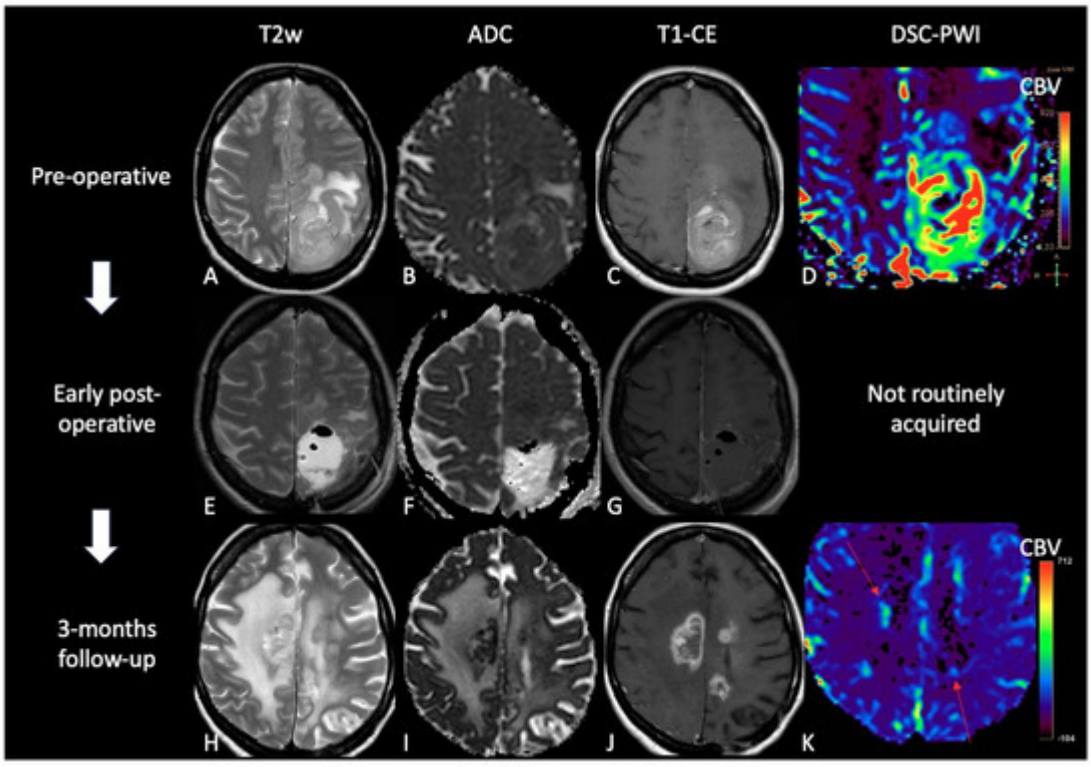

Figure 4. Case of TP. (**A**,**E**,**H**): T2w axial images; (**B**,**F**,**I**) ADC maps; (**C**,**G**,**J**) post-contrast T1w images after contrast; (**D**,**K**) DSC-CBV maps. The upper row shows a left parietal GB, with low ADC, CE, and high perfusion values in the CBV map. In the middle row there are post-operative images of macroscopically complete tumor resection. The lower row shows images three months after Stupp treatment, highlighting the appearance of tissue with CE in different site from the surgical bed, with low ADC values and high rCBV values, suggesting TP.

3.4. Late Post-Treatment Alterations

3.4.1. Radiation Necrosis: Definition and Physiopathology

Radiation necrosis (RN) is a late-delayed complication that typically occurs 6–24 months post radiotherapy but can occur up to several years/decades [21]. There is neither clear evidence of nor consensus on the distinction between PsP and RN, as the physiopathology of the radio-induced lesions is dynamic and complex [24].

RN affects 5–40% of patients, and it appears like a space-occupying mass with associated neurological symptoms. Its physiopathological mechanisms are not clear but probably rely on vascular endothelial damage, glial and white matter damage, and the activation of the fibrinolytic enzyme system, which lead to cytotoxic and vasogenic edema, demyelination and tissue necrosis [18][21][24].

3.4.2. Imaging: Conventional and Advanced MRI Sequences

The distinction between RN and TP is often not possible with conventional MRI alone. More typical morphological features of RN are the “Swiss cheese” CE pattern and the involvement of septum pellucidum, whereas progressive enhancing enlargement with mass effect and involvement of the corpus callosum are more suggestive of TP. However, RN and TP can mimic each other and often coexist. Therefore, advanced MRI techniques are required to correctly interpret MRI findings [25][26].

DWI and DTI have been assessed to differentiate TP and/or residual tumor from RN; ADC values were noted to be higher in RN than in TP and like in PsP, some studies have demonstrated lower FA values in RN than in TP [21][27].

About PWI, rCBV value is actually the most used advanced MRI indicator in post-treatment tumor assessment; indeed, several studies have shown that rCBV is lower in RN than in TP (**Figure 5**) [21]. Similarly, Ktrans is significantly lower in RN than in TP too [28].

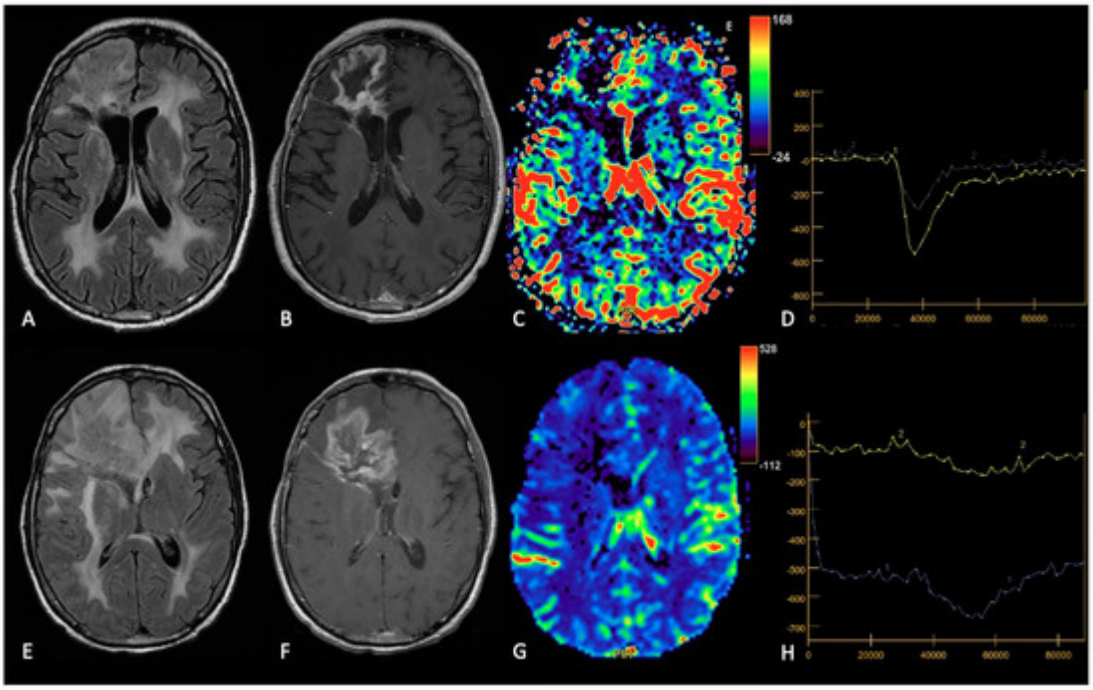

Figure 5. Example of RN. FLAIR (**A**,**E**), post-contrast T1w (**B**,**F**), DSC-CBV maps (**C**,**G**) and DSC- signal intensity/time curves (**D**,**H**).The upper row shows a case recurrent GB, with enhancing tissue surrounding the surgical cavity and increased rCBV values, without significative mass effect.After surgery and radio-chemotherapy, follow-up MRI (lower row) shows a large enhancing lesion with extensive vasogenic edema and mass effect, but without increased rCBV values. After another surgery, the histological showed radiation necrosis without tumor recurrence.

4. MRI Findings during Second-Line Therapy

Therapeutic choices in recurrent GB are still debated, and no data-driven guidelines are available to ease clinical decisions. Some treatment options have been proposed, including re-operation, re-irradiation, and systemic therapy, alone or in combination [29][30], but the choice of second-line treatment depends on several factors, such as the patient's overall health, the time to disease recurrence, the location, size and extent of the recurrent tumor, the response to previous treatments, the molecular and methylation status of the tumor, and the toxicity profile of the drug [30].

Usually, in the case of local recurrence, surgical resection precedes chemotherapy and less frequently re-irradiation, while in case of diffuse recurrence, systemic therapy is the first choice [30][31][32].

The available systemic treatments range from the oldest and commonly used chemotherapeutic agents, including lomustine (CCNU) given as a single agent or given in combination (PCV regimen) or re-challenge with TMZ [33][34], to novel targeted antiangiogenic and anti-growth-factor agents (e.g., bevacizumab and regorafenib) [35][36][37][38]. However, to date, their effectiveness in terms of length of OS remains still debated.

The effects of treatment impact on radiologic phenotypes and the interpretation of MRI abnormalities following the treatment failure remains the main diagnostic challenge. In addition, the introduction of novel antiangiogenic and anti-growth factor agents, such as bevacizumab (BEV) and regorafenib (REG), showed peculiar MRI patterns that required a revision of RANO criteria, including T2w/FLAIR lesions as a new criterion for glioma progression [39]. However, the revised evaluation criteria, based on conventional MR imaging alone, has also shown its weaknesses in differentiating non-enhancing progressive tumors from other causes of hyperintensity in T2w/FLAIR sequences, such as vasogenic edema, leukoencephalopathies, and microvascular ischemic spots. Advanced MRI sequences (DWI, PWI, and MRS) have demonstrated their usefulness in overcoming this problem, improving the assessment of treatment response in GB, by extending the existing RANO criteria [40].

The drug-related MR features/patterns of recurrence are grouped in two main categories according to currently approved treatments: traditional chemotherapeutic agents (e.g., TMZ, lomustine, and PCV) and novel targeted antiangiogenic agents (BEV and REG).

In the former group the recurrence pattern looks like the common MRI features of disease progression: increased T2w/FLAIR signal abnormality (due to edema and tumor infiltration) and increased CE according to standard criteria RANO, restricted DWI, and increased rCBV. On the other hand, the novel therapies, at the first follow-up, led to a dramatic reduction in the tumor CE as well as reduction in edema on MRI (“called” pseudoresponse) and, at progression, to an increase in non-enhancing T2w/FLAIR abnormalities. In this latter group, these effects are due to the stabilization of the immature and friable vasculature of the tumor and the decrease in the rate of microvascular proliferation and the effects on BBB permeability [41].

However, although the patterns of recurrence of novel targeted antiangiogenic agents (BEV and REG) may look similar, they differ because of their different ways of action.

BEV is a humanized monoclonal antibody directed against vascular endothelial growth factor (VEGF) [42][43], while REG is an orally available multikinase inhibitor with several molecular targets involved in angiogenesis (VEGFR1–3 and TIE2), oncogenesis (KIT, RET, RAF1, and BRAF) and maintenance of the tumoral microenvironment (PDGFR and FGFR) [44][45][46]. Their distinctive patterns may be appraisable by using combined standard and advanced MRI modalities, and below, the main specific MR patterns of failure under BEV and REG treatment are reported.

5.1. Introduction

Radiomics is a promising approach that can contribute to precision medicine by quantitatively analyzing clinical imaging arrays and utilizing artificial intelligence (AI) methods to improve the objectivity, accuracy, and the automation of radiological diagnoses. Machine learning (ML), a subfield of AI, can create computational models that can achieve astonishing results in aiding clinical decisions, by training the model with datasets.

Due to limited access to private and customized high-quality labeled brain tumor datasets, which are typically owned and protected by medical institutions, public datasets play a crucial role in providing an equal platform for ML researchers to train and compare the outcomes of their models. In the field of neuro-oncology, one of the most

widely used public image datasets is the Brain Tumor Segmentation (BraTS) challenge, organized by the Medical Image Computing and Computer Assisted Interventions (MICCAI) and other professional organizations since 2012. As of July 2023, the latest version, BraTS 2023, comprises more than 4500 brain tumor cases/patients, divided into three subsets: training, validation, and testing. Only the training and validation subsets are publicly accessible, and they include multimodal 3D MRI scans (T1, T1-CE, T2w, FLAIR) for each case. Other commonly used datasets include The Cancer Imaging Archive (TCIA) and The Whole Brain Atlas by Harvard Medical School [47].

Most AI techniques employed in brain tumor radiomic studies utilize supervised ML, which trains a model to predict a target variable from a set of predictive variables (data samples, taken from private or public databases), with the help of labels/annotations and a loss function (a mathematical function that measures the error between predicted and actual values in a machine learning model, and so how well the algorithm works; during training, the aim is to minimize this “loss” between the predicted and target outputs).

Recently, convolutional neural network (CNN)-based deep learning (DL) has gained popularity in neuro-oncology imaging due to its scalability and ability to extract local and global features (**Figure 6**) [47].

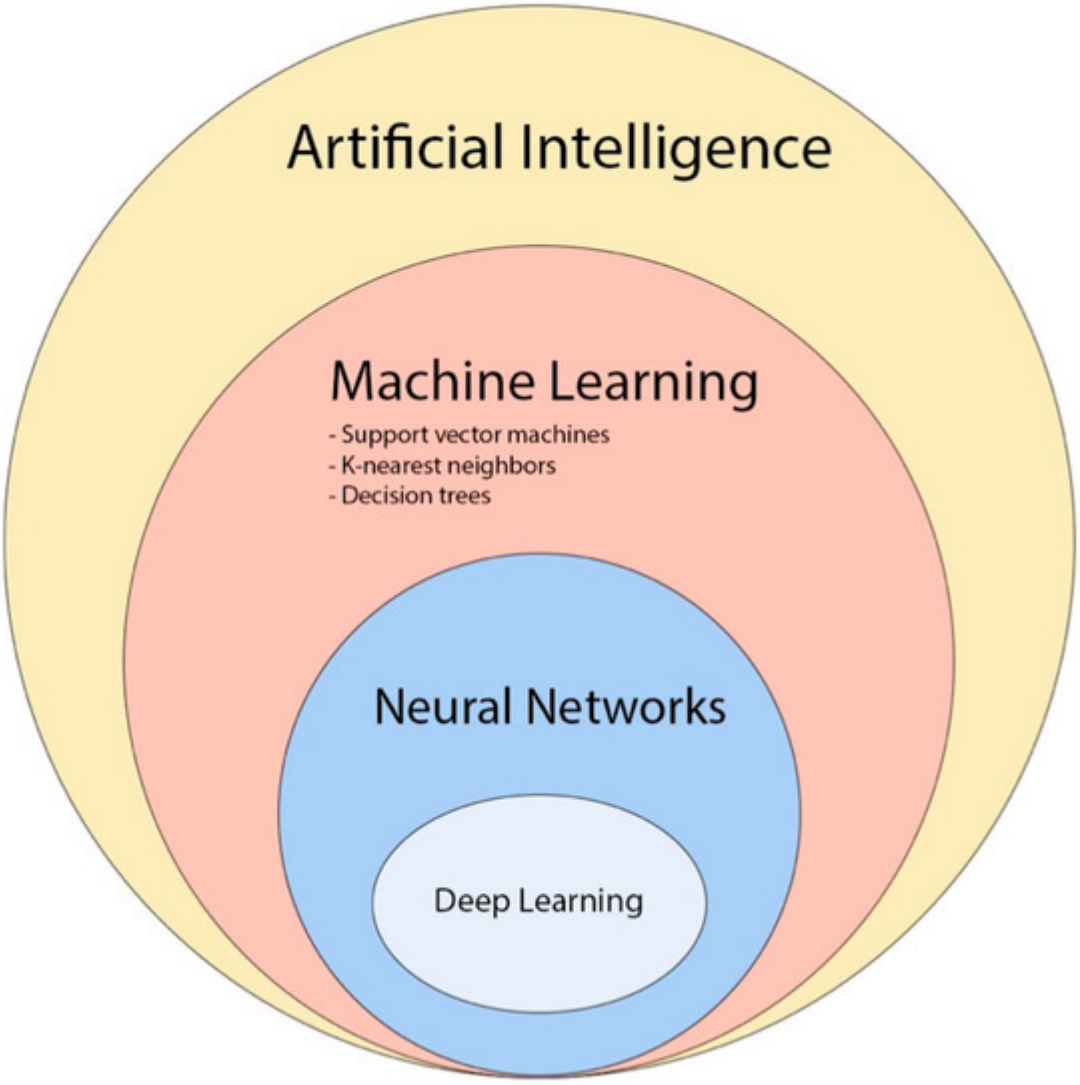

Figure 6. The diagram provides an overview of the various concepts and subfields related to artificial intelligence and how they are related with each other [48].

5.2. TP vs. Treatment-Related Changes

In the last decade, ML algorithms achieved interesting results that may aid in the follow-up management of treated GB patients in the near future and, more specifically, in differentiating treatment effects versus recurrent disease/true progression and in OS prediction.

As said, the interpretation of conventional MRI may pose a challenge in distinguishing tumor recurrence from RN and PsP, but an accurate differentiation between these entities is critical for treatment decisions during follow-up. Advanced MRI modalities are useful, but they are not always available, and their processing is time consuming and requires expertise. From this point of view, AI can be a tool to arrive at a faster and more objective diagnosis.

5.3. Overall Survival

Radiomic analysis has been shown to also provide more objective and accurate prediction of disease prognosis compared to conventional survival prediction based on clinical information, which is of great clinical importance and could benefit both treatment planning and patient care. Sanghani et al. utilized an SVM ML model to analyze texture, shape, volumetric features, and patient age derived from multimodal MRI data (T1-CE, T2, and FLAIR) of 173 patients to perform binary and multiclass OS prediction with accuracies of 0.987 and 0.89, respectively [49].

5.4. Prediction of Tumor Invasion and Recurrence

Another growing subfield of AI application in GB and high-grade gliomas (HGG) is the prediction of tumor invasion and recurrence.

One of the difficulties in treating GB lies in the inability to detect the cancer's invasive region beyond the contrast-enhancing tumor, since neoplastic cells infiltrate the non-enhancing peritumoral area, leading to high rate of local progression. Recent evidence suggests that extending the surgical resection of GB beyond the contrast-enhancing region could enhance patient survival. However, enlarging surgical margins may not always be feasible due to the risk of post-operative neurological deficits when the peritumor extends to critical areas [50]. The challenge arises from the fact that conventional MRI often fails to visually differentiate a non-enhancing tumor from vasogenic edema, despite specific radiological criteria. AI could help radiologists in this distinction, thanks to its ability to see changes non perceptible to the human eye, and thus can lead to new and targeted surgical limits and targets for radiotherapy.

References

1. Horbinski, C.; Nabors, L.B. NCCN Guidelines® Insights: Central Nervous System Cancers, Version 2.2022. J. Natl. Compr. Cancer Netw. 2023, 21, 12–20.
2. Weller, M.; van den Bent, M.; Preusser, M.; Le Rhun, E.; Tonn, J.C.; Minniti, G.; Bendszus, M.; Balana, C.; Chinot, O.; Dirven, L.; et al. EANO guidelines on the diagnosis and treatment of diffuse gliomas of adulthood. Nat. Rev. Clin. Oncol. 2021, 18, 170–186.
3. Aldave, G.; Tejada, S.; Pay, E.; Marigil, M.; Bejarano, B.; Idoate, M.A.; Díez-Valle, R. Prognostic value of residual fluorescent tissue in glioblastoma patients after gross total resection in 5-aminolevulinic Acid-guided surgery. Neurosurgery 2013, 72, 915–920.
4. Bette, S.; Gempt, J.; Huber, T.; Boeckh-Behrens, T.; Ringel, F.; Meyer, B.; Zimmer, C.; Kirschke, J.S. Patterns and Time Dependence of Unspecific Enhancement in Postoperative Magnetic Resonance Imaging After Glioblastoma Resection. World Neurosurg. 2016, 90, 440–447.
5. Brown, T.J.; Brennan, M.C.; Li, M.; Church, E.W.; Brandmeir, N.J.; Rakszawski, K.L.; Patel, A.S.; Rizk, E.B.; Suki, D.; Sawaya, R.; et al. Association of the Extent of Resection with Survival in Glioblastoma: A Systematic Review and Meta-analysis. JAMA Oncol. 2016, 2, 1460–1469.
6. Albert, F.K.; Forsting, M.; Sartor, K.; Adams, H.P.; Kunze, S. Early postoperative magnetic resonance imaging after resection of malignant glioma: Objective evaluation of residual tumor and its influence on regrowth and prognosis. Neurosurgery 1994, 34, 45–60.
7. Ekinci, G.; Akpınar, I.N.; Baltacıoglu, F.; Erzen, C.; Kılıc, T.; Elmacı, I.; Pamir, N. Early postoperative magnetic resonance imaging in glial tumors: Prediction of tumor regrowth and recurrence. Eur. J. Radiol. 2003, 45, 99–107.
8. Forsting, M.; Albert, F.K.; Kunze, S.; Adams, H.P.; Zenner, D.; Sartor, K. Extirpation of glioblastomas: MR and CT follow-up of residual tumor and regrowth patterns. AJNR Am. J. Neuroradiol. 1993, 14, 77–87.
9. Wen, P.Y.; Macdonald, D.R.; Reardon, D.A.; Cloughesy, T.F.; Sorensen, A.G.; Galanis, E.; Degroot, J.; Wick, W.; Gilbert, M.R.; Lassman, A.B.; et al. Updated response assessment criteria for high-grade gliomas: Response assessment in neuro-oncology working group. J. Clin. Oncol. 2010, 28, 1963–1972.
10. Lescher, S.; Schniewindt, S.; Jurcoane, A.; Senft, C.; Hattingen, E. Time window for postoperative reactive enhancement after resection of brain tumors: Less than 72 h. J. Neurosurg. 2014, 37, E3.
11. Booth, T.C.; Luis, A.; Brazil, L.; Thompson, G.; Daniel, R.A.; Shuaib, H.; Ashkan, K.; Pandey, A. Glioblastoma post-operative imaging in neuro-oncology: Current UK practice (GIN CUP study). Eur. Radiol. 2021, 31, 2933–2943.
12. Ellingson, B.M.; Bendszus, M.; Boxerman, J.; Barboriak, D.; Erickson, B.J.; Smits, M.; Nelson, S.J.; Gerstner, E.; Alexander, B.; Goldmacher, G.; et al. Consensus recommendations for a

standardized Brain Tumor Imaging Protocol in clinical trials. Neuro-Oncology 2015, 17, 1188–1198.

13. Elster, A.D.; DiPersio, D.A. Cranial postoperative site: Assessment with contrast-enhanced MR imaging. Radiology 1990, 174, 93–98.
14. Garcia-Ruiz, A.; Naval-Baudin, P.; Ligero, M.; Pons-Escoda, A.; Bruna, J.; Plans, G.; Calvo, N.; Cos, M.; Majós, C.; Perez-Lopez, R. Precise enhancement quantification in post-operative MRI as an indicator of residual tumor impact is associated with survival in patients with glioblastoma. Sci. Rep. 2021, 11, 695.
15. Stupp, R.; Mason, W.P.; Van den Bent, M.J.; Weller, M.; Fisher, B.; Taphoorn, M.J.; Belanger, K.; Brandes, A.; Marosi, C.; Bogdahn, U.; et al. Radiotherapy plus concomitant and adjuvant temozolomide for glioblastoma. N. Engl. J. Med. 2005, 352, 987–996.
16. Mrugala, M.M.; Chamberlain, M.C. Mechanisms of disease: Temozolomide and glioblastoma—Look to the future. Nat. Clin. Pract. Oncol. 2008, 5, 476–486.
17. Brandsma, D.; Stalpers, L.; Taal, W.; Sminia, P.; Van den Bent, M.J. Clinical features, mechanisms, and management of pseudoprogression in malignant gliomas. Lancet Oncol. 2008, 9, 453–461.
18. Zikou, A.; Sioka, C.; Alexiou, G.A.; Fotopoulos, A.; Voulgaris, S.; Argyropoulou, M.I. Radiation Necrosis, Pseudoprogression, Pseudoresponse, and Tumor Recurrence: Imaging Challenges for the Evaluation of Treated Gliomas. Contrast Media Mol. Imaging 2018, 2018, 6828396.
19. Turnquist, C.; Harris, B.T.; Harris, C.C. Radiation-induced brain injury: Current concepts and therapeutic strategies targeting neuroinflammation. Neurooncol. Adv. 2020, 2, vdaa057.
20. Provenzale, J.M.; Mukundan, S.; Barboriak, D.P. Diffusion-weighted and Perfusion MR Imaging for Brain Tumor Characterization and Assessment of Treatment Response. Radiology 2006, 239, 632–649.
21. Qin, D.; Yang, G.; Jing, H.; Tan, Y.; Zhao, B.; Zhang, H. Tumor Progression and Treatment-Related Changes: Radiological Diagnosis Challenges for the Evaluation of Post Treated Glioma. Cancers 2022, 14, 3771.
22. Parvez, K.; Parvez, A.; Zadeh, G. The Diagnosis and Treatment of Pseudoprogression, Radiation Necrosis and Brain Tumor Recurrence. Int. J. Mol. Sci. 2014, 15, 11832–11846.
23. Martucci, M.; Russo, R.; Schimperna, F.; D'Apolito, G.; Panfili, M.; Grimaldi, A.; Perna, A.; Ferranti, A.M.; Varcasia, G.; Giordano, C.; et al. Magnetic Resonance Imaging of Primary Adult Brain Tumors: State of the Art and Future Perspectives. Biomedicines 2023, 11, 364.
24. Nichellia, L.; Casagranda, S. Current emerging MRI tools for radionecrosis and pseudoprogression diagnosis. Curr. Opin. Oncol. 2021, 33, 597–607.

25. Malik, D.G.; Rath, T.J.; Urcuyo Acevedo, J.C.; Canoll, P.D.; Swanson, K.R.; Boxerman, J.L.; Chad Quarles, C.; Schmainda, K.M.; Burns, T.C.; Hu, L.S. Advanced MRI Protocols to Discriminate Glioma from Treatment Effects: State of the Art and Future Directions. Front. Radiol. 2022, 2, 809373.
26. Shah, R.; Vattoth, S.; Jacob, R.; Manzil, F.F.P.; O'Malley, J.P.; Borghei, P.; Patel, B.N.; Curé, J.K. Radiation Necrosis in the Brain: Imaging Features and Differentiation from Tumor Recurrence. Radiographics 2012, 32, 1343–1359.
27. Razek, A.A.K.A.; El-Serougy, L.; Abdelsalam, M.; Gaballa, G.; Talaat, M. Differentiation of residual/recurrent gliomas from postradiation necrosis with arterial spin labeling and diffusion tensor magnetic resonance imaging-derived metrics. Neuroradiology 2018, 60, 169–177.
28. Nael, K.; Bauer, A.H.; Hormigo, A.; Lemole, M.; Germano, I.M.; Puig, J.; Baldassarre, S. Multiparametric MRI for Differentiation of Radiation Necrosis from Recurrent Tumor in Patients with Treated Glioblastoma. Am. J. Roentgenol. 2018, 210, 18–23.
29. Weller, M.; Perry, T.J.R.; Wick, W. Standards of care for treatment of recurrent glioblastoma are we there yet? Neuro-Oncology 2013, 15, 4–27.
30. Tosoni, A.; Franceschi, A.; Poggi, R.; Brandes, A.A. Relapsed Glioblastoma: Treatment Strategies for Initial and Subsequent Recurrences. Curr. Treat. Options Oncol. 2016, 17, 49.
31. Bloch, O.; Han, S.J.; Cha, S.; Sun, M.Z.; Aghi, M.K.; McDermott, M.W.; Berger, M.S.; Parsa, A.T. Impact of extent of resection for recurrent glioblastoma on overall survival: Clinical article. J. Neurosurg. 2012, 117, 1032–1038.
32. Gregucci, F.; Surgo, A.; Carbonara, R.; Laera, L.; Ciliberti, M.P.; Gentile, M.A.; Caliandro, M.; Sasso, N.; Bonaparte, I.; Fanelli, V.; et al. Radiosurgery and Stereotactic Brain Radiotherapy with Systemic Therapy in Recurrent High-Grade Gliomas: Is It Feasible? Therapeutic Strategies in Recurrent High-Grade Gliomas. J. Pers. Med. 2022, 12, 1336.
33. Afonso, M.; Brito, M.A. Therapeutic Options in Neuro-Oncology. Int. J. Mol. Sci. 2022, 11, 5351.
34. Ahn, S.; Il Kim, Y.; Shin, J.Y.; Park, J.S.; Yoo, C.; Lee, Y.S.; Hong, Y.; Jeun, S.; Yang, S.H. Clinical feasibility of modified procarbazine and lomustine chemotherapy without vincristine as a salvage treatment for recurrent adult glioma. Oncol. Lett. 2022, 23, 114.
35. Hasselbalch, B.; Lassen, U.; Hansen, S.; Holmberg, M.; Sørensen, M.; Kosteljanetz, M.; Broholm, H.; Stockhausen, M.; Skovgaard Poulsen, H. Cetuximab, bevacizumab, and irinotecan for patients with primary glioblastoma and progression after radiation therapy and temozolomide: A phase II trial. Neuro-Oncology 2010, 12, 508–516.
36. Lau, D.; Magill, S.T.; Aghi, M.K. Molecularly targeted therapies for recurrent glioblastoma: Current and future targets. Neurosurg. Focus 2014, 37, E15.

37. Friedman, H.S.; Prados, M.D.; Wen, P.Y.; Mikkelsen, T.; Schiff, D.; Abrey, L.E.; Yung, W.K.A.; Paleologo, N.; Nicholas, M.K.; Jensen, R.; et al. Bevacizumab alone and in combination with irinotecan in recurrent glioblastoma. J. Clin. Oncol. 2009, 27, 4733–4740.
38. Lombardi, G.; De Salvo, G.L.; Brandes, A.A.; Eoli, M.; Rudà, R.; Faedi, M.; Lolli, I.; Pace, A.; Daniele, B.; Pasqualetti, F.; et al. Regorafenib compared with lomustine in patients with relapsed glioblastoma (REGOMA): A multicentre, open-label, randomised, controlled, phase 2 trial. Lancet Oncol. 2019, 20, 110–119.
39. Gahrmann, R.; Bent, M.; Holt, B.; Vernhout, R.M.; Taal, W.; Vos, M.; Groot, J.C.; Beerepoot, L.V.; Buter, J.; Flach, Z.H.; et al. Comparison of 2D (RANO) and volumetric methods for assessment of recurrent glioblastoma treated with bevacizumab-a report from the BELOB trial. Neuro-Oncology 2017, 19, 853–861.
40. Ellingson, B.M.; Cloughesy, T.F.; Lai, A.; Nghiemphu, P.L.; Lalezari, S.; Zaw, T.; Motevalibashinaeini, K.; Mischel, P.S.; Pope, W.B. Quantification of edema reduction using differential quantitative T2 (DQT2) relaxometry mapping in recurrent glioblastoma treated with bevacizumab. J. Neurooncol. 2012, 106, 111–119.
41. Nowosielski, M.; Wiestler, B.; Goebel, G.; Hutterer, M.; Schlemmer, H.P.; Stockhammer, G.; Wick, W.; Bendszus, M.; Radbruch, A. Progression types after antiangiogenic therapy are related to outcome in recurrent glioblastoma. Neurology 2014, 82, 1684–1692.
42. Jain, R.K. Normalization of tumor vasculature: An emerging concept in antiangiogenic therapy. Science 2005, 307, 58–62.
43. Macdonald, D.R.; Cascino, T.L.; Schold, S.C., Jr.; Cairncross, J.G. Response criteria for phase II studies of supratentorial malignant glioma. J. Clin. Oncol. 1990, 8, 1277–1280.
44. Abou-Elkacem, L.; Arns, S.; Brix, G.; Gremse, F.; Zopf, D.; Kiessling, F.; Lederle, W. Regorafenib inhibits growth, angiogenesis, and metastasis in a highly aggressive, orthotopic colon cancer model. Mol. Cancer Ther. 2013, 12, 1322–1331.
45. Wilhelm, S.M.; Dumas, J.; Adnane, L.; Lynch, M.; Carter, C.A.; Schütz, G.; Thierauch, K.; Zopf, D. Regorafenib (BAY 73-4506): A new oral multikinase inhibitor of angiogenic, stromal and oncogenic receptor tyrosine kinases with potent preclinical antitumor activity. Int. J. Cancer. 2011, 129, 245–255.
46. Zeiner, P.S.; Kinzig, M.; Divé, I.; Maurer, G.D.; Filipski, K.; Harter, P.N.; Senft, C.; Bähr, O.; Hattingen, E.; Steinbach, J.P.; et al. Regorafenib CSF Penetration, Efficacy, and MRI Patterns in Recurrent Malignant Glioma Patients. J. Clin. Med. 2019, 8, 2031.
47. Zhu, M.; Li, S.; Kuang, Y.; Hill, V.B.; Heimberger, A.B.; Zhai, L.; Zhai, S. Artificial intelligence in the radiomic analysis of glioblastomas: A review, taxonomy, and perspective. Front. Oncol. 2022, 12, 924245.

48. Rudie, J.D.; Rauschecker, A.M.; Bryan, R.N.; Davatzikos, C.; Mohan, S. Emerging Applications of Artificial Intelligence in Neuro-Oncology. Radiology 2019, 290, 607–618.
49. Sanghani, P.; Ang, B.T.; King, N.K.K.; Ren, H. Overall survival prediction in glioblastoma multiforme patients from volumetric, shape and texture features using machine learning. Surg. Oncol. 2018, 27, 709–714.
50. Rakovec, M.; Khalafallah, A.M.; Wei, O.; Day, D.; Sheehan, J.P.; Sherman, J.H.; Mukherjee, D. A consensus definition of supratotal resection for anatomically distinct primary glioblastoma: An AANS/CNS Section on Tumors survey of neurosurgical oncologists. J. Neurooncol. 2022, 159, 233–242.